

# Crystal structure of the DNA-binding domain of BldD, a central regulator of aerial mycelium formation in *Streptomyces coelicolor* A3(2)

In-Kwon Kim,<sup>1‡</sup> Chang-Jin Lee,<sup>1‡</sup> Min-Kyu Kim,<sup>1</sup>  
Jeong-Mok Kim,<sup>1</sup> Ji-Hye Kim,<sup>1</sup> Hyung-Soon Yim,<sup>1</sup>  
Sun-Shin Cha<sup>2\*</sup> and Sa-Ouk Kang<sup>1†</sup>

<sup>1</sup>Laboratory of Biophysics, School of Biological Sciences,  
and Institute of Microbiology, Seoul National University,  
Seoul 151-742, Republic of Korea.

<sup>2</sup>Beamline Division, Pohang Accelerator Laboratory,  
Pohang 790-784, Republic of Korea.

## Summary

**BldD is a central regulator of the developmental process in *Streptomyces coelicolor*. The 1.8 Å resolution structure of the DNA-binding domain of BldD (BldDN) reveals that BldDN forms a compact globular domain composed of four helices ( $\alpha$ 1– $\alpha$ 4) containing a helix-turn-helix motif ( $\alpha$ 2– $\alpha$ 3) resembling that of the DNA-binding domain of lambda repressor. The BldDN/DNA complex model led us to design a series of mutants, which revealed the important role of  $\alpha$ 3 and the 'turn' region between  $\alpha$ 2 and  $\alpha$ 3 for DNA recognition. Based on the fact that BldD occupies two operator sites of *bldN* and *whiG* and shows significant disparity in the affinity toward the two operator sites when they are disconnected, we propose a model of cooperative binding, which means that the binding of one BldD dimer to the high affinity site facilitates that of the second BldD dimer to the low affinity site. In addition, structural and mutational investigation reveals that the Tyr62Cys mutation, found in the first-identified *bldD* mutant, can destabilize BldD structure by disrupting the hydrophobic core.**

## Introduction

Streptomyces, filamentous soil bacteria, are industrially important because they produce many beneficial metabolites such as antibiotics, antiparasitic agents, herbicides and pharmacologically active metabolites (e.g. immunosuppressants) (Hodgson, 2000). In addition, their morpho-

logical differentiation, which involves complex regulation of gene expression, makes them unique among bacteria. The developmental process begins with the formation of multigenomic aerial mycelia that grow out into the air, constituting a fuzzy layer on the colony surface, and finally unigenomic spores are generated through the multiple septation of aerial hyphae (Chater, 1993, 1998; Kelemen and Buttner, 1998).

Two main classes of genes, *whi* and *bld* genes, that are requisite for the morphological development have been identified in *Streptomyces coelicolor*, which is the most studied member of the genus (Chater, 1972, 1998). The *whi* genes, whose mutations yield 'white' aerial mycelium due to the lack of the grey spore pigment, are essential for the spore maturation in aerial hyphae (Chater, 1972). Mutations in the *bld* genes cause the loss of aerial hyphae and have a shiny, 'bald' phenotype (Merrick, 1976; Willey *et al.*, 1993; Nodwell *et al.*, 1996). Moreover, the *bld* mutants show pleiotropic effects, including defects in carbon catabolite repression and in cell–cell signalling, and sometimes inhibition of antibiotic production (Merrick, 1976; Champness, 1988; Willey *et al.*, 1993; Pope *et al.*, 1996; Kelemen and Buttner, 1998; Nodwell *et al.*, 1999).

So far, many *bld* mutants, including *bldA*, *bldB*, *bldC*, *bldD*, *bldF*, *bldG*, *bldH*, *bldI*, *bldK* and *bldM*, have been identified. These mutants are known to be unable to produce a small hydrophobic molecule, SapB (Spore-associated protein) that contributes to aerial hyphae formation by reducing the surface tension at the colony surface (Willey *et al.*, 1991; Tillotson *et al.*, 1998). Interestingly, when certain pairs of *bld* mutants are grown on rich media in close proximity, one mutant can trigger aerial hyphae formation of the other mutant (Willey *et al.*, 1991; Willey *et al.*, 1993; Tillotson *et al.*, 1998; Nodwell *et al.*, 1999; Molle and Buttner, 2000). This so-called extracellular complementation is always unidirectional, and can be explained by assuming the hierarchical cascade of intercellular signals for aerial hyphae formation: [*bldJ*] < [*bldK* – *bldL*] < [*bldA* – *bldH*] < [*bldG*] < [*bldC*] < [*bldM* – *bldD*].

That is, one mutant that is higher in the hierarchy and acts as a donor can give signals to the other mutant acting as a recipient through unidentified signalling mechanism, and thus render the recipient mutant to

Accepted 24 March, 2006. For correspondence. \*E-mail chajung@postech.ac.kr; Tel. (+82) 54 279 1563; Fax (+82) 54 279 1599. †E-mail kangsaou@snu.ac.kr; Tel. (+82) 2880 6703; Fax (+82) 2888 4911. ‡Both authors equally contributed to this work.

restore the ability to produce a morphogenic peptide, SapB. The *bldD* mutant stands on top of the complementation hierarchy and is able to complement extracellularly all of the known *bld* mutants except for itself and the *bldM* mutant that takes the same position in the hierarchy as the *bldD* mutant (Willey *et al.*, 1993; Nodwell *et al.*, 1996).

*Streptomyces coelicolor* *ram* gene cluster (*ramA*, *ramB*, *ramC*, *ramR* and *ramS*) has also been revealed to be required for the erection of aerial hyphae (Ma and Kendall, 1994). These genes accelerated the formation of aerial hyphae when introduced into *Streptomyces lividans* (Ma and Kendall, 1994), and *ramC*-, *ramS*- and *ramR*-deleted mutants exhibited a severe defect in aerial hyphae formation (O'Connor *et al.*, 2002). Recently, Kodani *et al.* (2004) demonstrated that SapB is a lantibiotic-like peptide derived from RamS, strongly suggesting that the expression of *ram* gene cluster is under the control of the *bld* gene-dependent extracellular cascades. Consistently, the *ram* genes were not transcribed in the *bld* mutants (*bldA*, *bldB*, *bldH* and *bldD*) (Keijsers *et al.*, 2002). Considering the extracellular complementation hierarchy, therefore, it can be assumed that the *bldD* gene exists at the highest position in *bld* and *ram* gene-mediated signalling cascades and roles as a central regulator of aerial hyphae formation in *S. coelicolor*.

The *bldD* gene product, BldD, consists of 167 amino acids and exists mainly as a dimer in solution (Elliot *et al.*, 2003). The first-identified *bldD* mutant has a point mutation at position 62 from Tyr to Cys (Elliot *et al.*, 1998). Elliot *et al.* (2003) reported that constructed *bldD* null mutant showed the same phenotype as the *bldD* point mutant, indicating that the point mutation (Y62C) completely abolished the function of BldD. Analysis of the BldD sequence using PFAM search (Bateman *et al.*, 1999; Kelemen *et al.*, 2001) revealed that BldD contains an XRE (Xenobiotic Response Element) type of helix-turn-helix (HTH) motif at its N-terminus. This family of transcription factors includes lambda repressor (Maniatis and Ptashne, 1973; Maniatis *et al.*, 1975) and *Bacillus subtilis* sporulation repressor SinR (Gaur *et al.*, 1986), which operate at crucial checkpoints where the biological fate is determined. For example, the lambda repressor cooperatively binds to the lytic promoter and prevents the expression of genes required for lytic growth (Meyer *et al.*, 1980). BldD also operates as a repressor at developmental checkpoint and binds to several target sites with imperfect inverted repeat (Elliot *et al.*, 2001). In fact, BldD binds to its own promoter (Elliot and Leskiw, 1999; Elliot *et al.*, 2001) and regulatory regions of several developmental key genes such as *bldN* encoding a sigma factor required for the formation of aerial hyphae and the transcription of *bldM* (Bibb *et al.*, 2000), and *whiG* which encodes a sigma factor that plays a critical role in sporulation (Chater *et al.*, 1989). In addition,

BldD binds to the promoters of *sigH* encoding the sigma factor associated with stress responses (Kelemen *et al.*, 2001) and *bdtA* (= *BldD* target) whose function is still uncharacterized (Elliot *et al.*, 2001).

As an effort to gain a better elucidation of BldD function, we have determined the three dimensional structure of the N-terminal DNA-binding domain of BldD (BldDN) from *Streptomyces coelicolor* A3(2) at 1.8 Å resolution. This structure will provide an important framework for understanding how BldD recognizes multiple promoter sites and thus regulates their transcription as well as how the point mutation at position 62 eliminates the whole function of BldD.

## Results and discussion

### Overview of BldDN monomer structure

Out of the total 79 amino acids in native BldDN, residues 2–71 are visible in the crystal structure. BldDN adopts a compact globular structure composed of four helices (Fig. 1A), which is stabilized by hydrophobic interactions among helices: Leu13 from  $\alpha 1$  (residues 3–20), Val27 from  $\alpha 2$  (residues 24–32), Trp35 from the turn between  $\alpha 2$  and  $\alpha 3$  (turn23), Val40 from  $\alpha 3$  (residues 37–45), Leu58, Phe61 and Tyr62 from  $\alpha 4$  (residues 51–62) form a hydrophobic core (Fig. 1B). The C-terminal loop (residues 65–71) takes part in the dimeric packing interactions in crystals (see *Dimerization of BldDN*) (Fig. 1A). Of the four helices,  $\alpha 2$  and  $\alpha 3$  constitute a classical HTH DNA-binding motif, and  $\alpha 1$  appears to form a structural scaffold that anchors  $\alpha 2$  and  $\alpha 3$  (Fig. 1A) (Harrison and Aggarwal, 1990). In this classical motif, the latter helix, often called a 'recognition helix', typically makes specific contacts with bases in the major groove of DNA. In BldDN, similarly,  $\alpha 3$  roles as the recognition helix (see *BldDN/DNA complex model*).

Structural homologue search using the program DALI (Holm and Sander, 1997) identified several homologues of BldDN, ascertaining that the three dimensional structure of BldDN is closely related to the XRE family of transcription factors. The highest homologue was the DNA-binding domain of lambda repressor (lambdaN) (Z-score of 9.3 and r.m.s.d. of 2.2 Å). The lambdaN (residues 1–93) contains five  $\alpha$  helices. Consistent with BldDN, the first four helices form a compact globular domain containing a classical HTH motif with  $\alpha 3$  as a recognition helix (Jordan and Pabo, 1988). Despite limited sequence identity between BldDN and lambdaN (~25%) (Fig. 2A), the structure of BldDN is well-superimposed onto that of lambdaN except for the additional helix ( $\alpha 5$ ) of lambdaN (Fig. 2B), proposing that BldD and lambda repressor could be related in their DNA-binding mode.

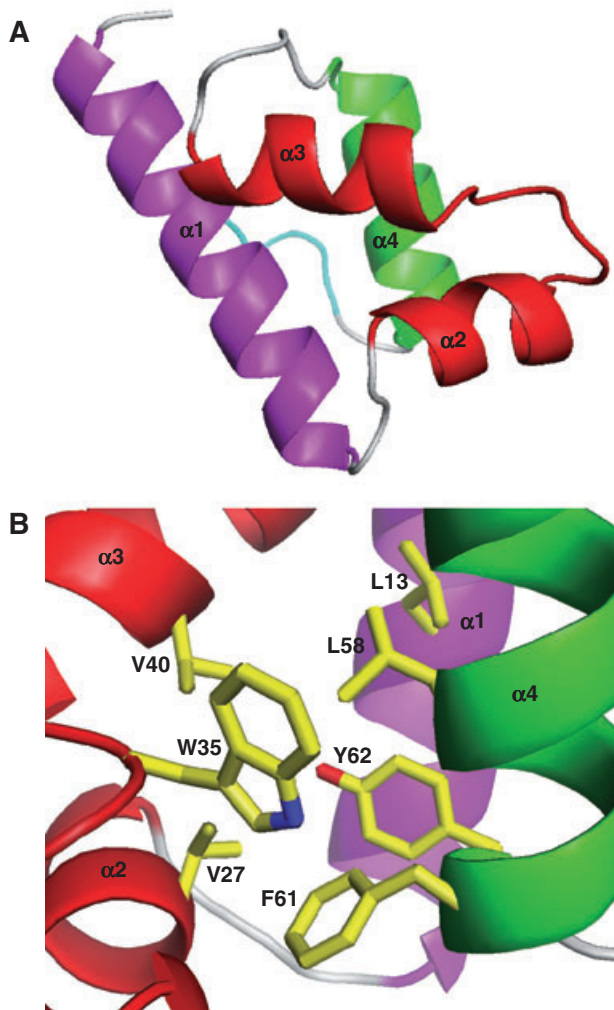


**Fig. 1.** Overall structure of BldDN. A. A ribbon diagram of BldDN monomer shown with secondary structures labelled. The helix-turn-helix motif is coloured red;  $\alpha 1$  and  $\alpha 4$  is coloured magenta and green respectively; loop is coloured light grey; the C-terminal loop that participates in the dimerization of BldDN is coloured cyan. B. A ribbon diagram showing the hydrophobic core of BldDN with secondary structures and important residues labelled.

#### Dimerization of BldDN

In general, transcription factors act as a dimer or tetramer, and BldD also binds to its own promoter as a dimer (Elliot *et al.*, 2003). The fact that BldDN retains its DNA-binding ability (Fig. 3A) and exists as a dimer in solution (Fig. 3B) arouses an interest in the dimerization of BldDN, and we can find weak dimeric contacts of BldDN in crystal packing. The C-terminal loop of BldDN of one subunit slightly extends out from the globular domain to form a dimer interface with that of the other subunit: the side chain of Leu70 of one subunit interacts with Val66' of the other, and similarly Val66 makes hydrophobic contacts with Leu70' (Fig. 4A). These two subunits are arranged with

respect to the twofold crystallographic symmetry in crystals.

However, these dimeric contacts of BldDN are not extensive (only 14.7% of surface is buried on dimerization), and the arrangement of the two HTH motifs of BldDN dimer observed in crystals is not effective to bind DNA. When two BldDN monomers were superimposed onto lambdaN/operator complex structure, the dimer interface of BldDN was disrupted (Fig. 4B). In addition, the dissociation constant ( $K_D$ ) of BldDN is 2.2-fold higher than wild-type BldD, indicating that the C-terminal domain contributes to the effective DNA binding of BldD (Fig. 3C). Therefore, the dimeric contacts of BldDN observed in crystals appear not to reflect the dimeric interactions of intact BldD, and instead the C-terminal domain of BldD, like lambda repressor, might mainly contribute to the dimerization of BldD. In lambda repressor, although stable lambdaN/DNA complex structure was reported (Beamer and Pabo, 1992), the C-terminal domain (residues 132–236) primarily mediates the dimerization of full-length lambda repressor (Bell and Lewis, 2001).

#### BldDN/DNA complex model

Structural similarity between BldDN and lambdaN led us to hypothesize that BldDN would be similar to lambdaN in terms of the DNA-binding mode. To get insights into the BldD–DNA interactions, we built a model of a DNA-bound BldDN by superimposing BldDN onto the lambdaN/DNA complex structure (Fig. 4B). According to this model which shows good geometric and electrostatic complementarity between BldDN and DNA,  $\alpha 3$  fits snugly into the major groove and makes direct interactions with DNA: the mainly basic and hydrophobic residues including Lys36 from turn23, and Val38, Ser42, Tyr43 and Arg45 from  $\alpha 3$ , contact directly DNA through hydrophobic or polar interactions (Fig. 4B and D). Supporting this model, the surface representation shows that hydrophobic and positive-charged residues are located along and around  $\alpha 3$  (Fig. 4C), indicating that these region possibly contacts bases and phosphate backbone.

#### Mutational analysis of the ability of full-length BldD to bind DNA based on the BldDN/DNA complex model

In the BldDN/DNA model, the recognition helix,  $\alpha 3$ , most extensively contacts the major groove of DNA (Fig. 4B). To further explore DNA recognition by BldD, We mutated five residues of  $\alpha 3$ , Val38, Val40, Ser42, Tyr43 and Arg45, to alanine, and tested the ability of single-site full-length BldD mutant to bind to four BldD-binding sites by electrophoretic mobility shift assay (EMSA) experiments (Fig. 5A).

As shown in Fig. 5A, substitution of Tyr43 and Arg45, both of which are predicted to interact with DNA from the BldDN/DNA complex model, with alanine resulted in

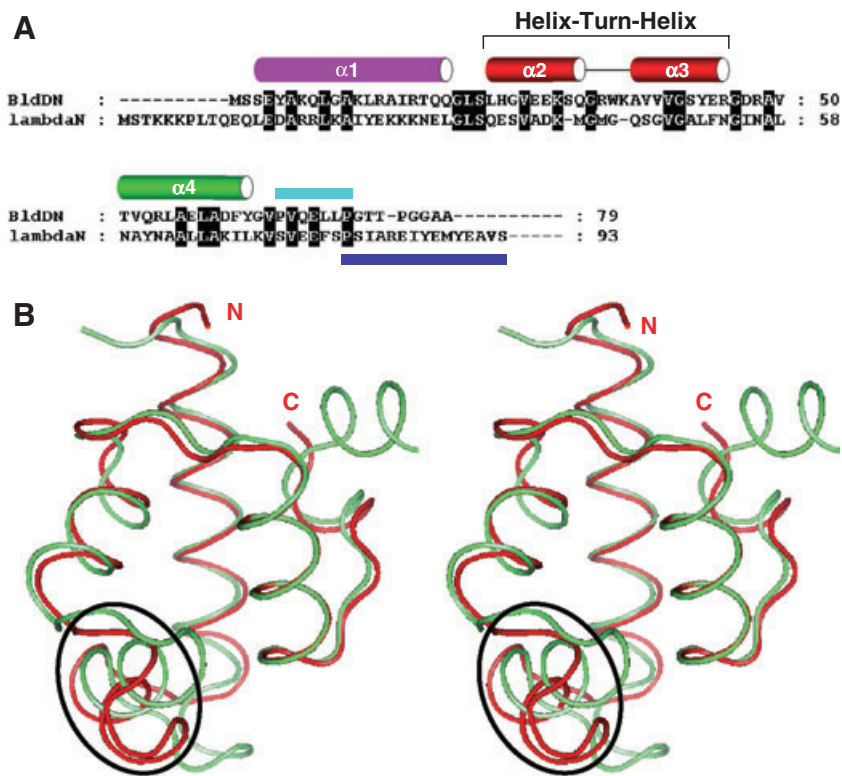


**Fig. 2.** Structural similarity to the DNA-binding domain of lambda repressor.

A. Structure based alignment of BldDN with lambdaN. The top of sequence alignment indicates secondary structure annotation of BldDN. The C-terminal loop that participates in the dimerization of BldDN is indicated by cyan bar. The additional helix of lambdaN compared with BldDN is indicated by blue bar. The colour scheme of white on black indicates the identical residue at a given position.

B. Stereo view of the superimposed structures of BldDN (red) and lambdaN (lime). N and C indicate the N- and C-termini of BldDN respectively. The four-residue 'turn' of BldDN, which is longer than the corresponding region of lambdaN, is highlighted by a black ellipse.

almost complete loss of DNA-binding activity. In contrast, S42A mutant exhibits a selective defect against four operator sites. In lambda repressor, Ser45 in the recognition helix, corresponding to Ser42 of BldD, directly contacts DNA by polar interaction, and S45A mutant failed to discriminate between base-pair changes at specific location of the operator site (Hochschild and Ptashne, 1986; Beamer and Pabo, 1992). Furthermore, Ser45 contacts the asymmetric operator site (consensus and non-consensus half) with two distinct conformations, suggesting an important role of Ser45 in the specific recognition of the asymmetric operator sites by lambda repressor. The seven known BldD-binding sites (Elliot *et al.*, 2001; Kelemen *et al.*, 2001) also consist of incomplete inverted repeat with relatively low sequence conservation. That is, BldD dimer would bind asymmetrically to them and  $\alpha 3$  of BldD is much likely to contribute to the discrimination and specific recognition of these variable sequences. The selective binding observed in S42A mutant indicates that this mutant protein has a defect in recognizing the sequence variation. Therefore, Ser42 can be assumed to be related to the specific recognition of multiple operator sites with incomplete inverted repeat by BldD.

Complete loss of DNA-binding activity was also observed in V40A mutant. Because Val40 appears to be simply involved in the hydrophobic core formation (Fig. 1B), it can be deduced that the correct hydrophobic core formation of BldD contributes to the protein function

possibly by providing a stable scaffold for DNA binding. The importance of the hydrophobic core will be additionally discussed (see *Mutational analysis of Tyr62 residue*).

#### Possible role of turn23 in DNA binding

In BldDN/DNA complex model, Lys36 of turn23 directly contacts the phosphate backbone of DNA (Fig. 4D). In addition, interestingly, large and positively charged residues such as Arg34, Trp35 and Lys36 are located at this turn23. To speculate the role of turn23, Arg34, Trp35 and Lys36 were mutated to alanine. The K36A mutant showed severe defect in its DNA-binding activity, as expected in the BldDN/DNA model (Fig. 5B). Selective and significant defects in DNA binding were observed in R34A, W35A and R34A/W35A mutants (Fig. 5B). These residues make extensive contacts with each other and residues mainly from  $\alpha 4$ : the bulky side chain of Trp35 stacks with the side chain of Arg34 in turn23, and makes hydrophobic contacts with Arg54, Leu58 and Phe61 from  $\alpha 4$  (Fig. 4E). These contacts appear to be of importance in maintaining proper conformation of turn23 for DNA binding. Therefore, substitution of Arg34 and Trp35 with alanine would affect the structure of turn23 interfering with the recognition of DNA.

The two helices of the prokaryotic HTH motif are generally connected by a short turn of three amino acids that starts from mainly glycine residue (Brennan and Matthews, 1989; Wintjens and Rooman, 1996). The lambda

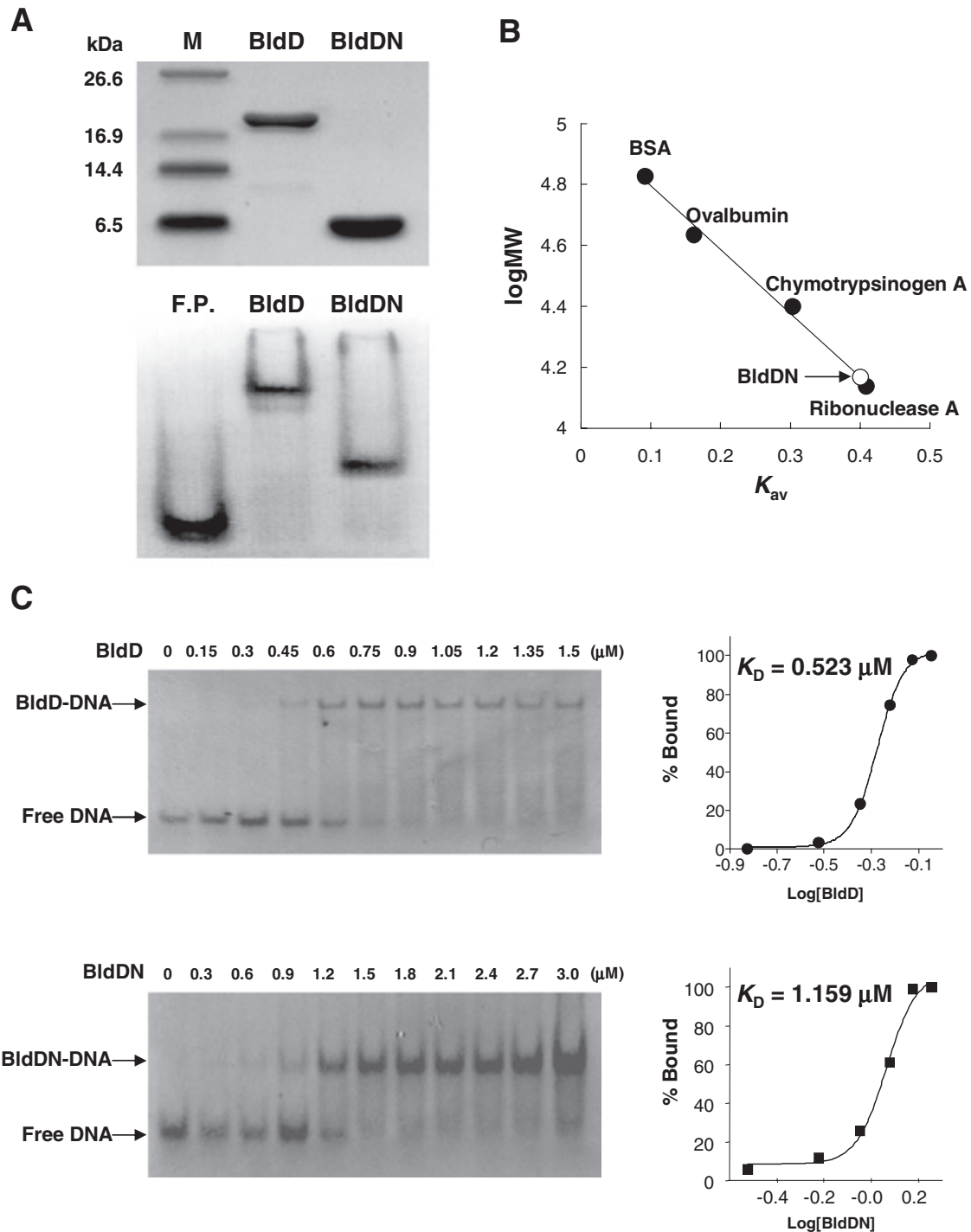


**Fig. 3.** Characterization of BldDN.

A. Purified BldDN retains its DNA-binding ability. Two micrograms of purified recombinant BldD and BldDN were applied on 15% Tris-tricine gel electrophoresis (top). EMSA experiment against *pblidD* was performed with equal amount of BldD and BldDN using 10% native gel containing  $1\times$  TBE (bottom). M indicates low molecular weight marker. F.P. indicates free probe of *pblidD*.

B. Determination of oligomeric state of BldDN. Oligomeric state of BldDN was analysed by gel filtration chromatography. Predicted molecular mass of BldDN (see *Experimental procedures*) is 14 673 Da ( $K_{av} = 0.40$ ), indicating that BldD exists as a dimer in solution.

C. Determination of the dissociation constant ( $K_D$ ) of BldD (top) and BldDN (bottom). EMSA experiments against *pblidD* were performed with 0.15–1.5  $\mu$ M of BldD (top left) or 0.3–3.0  $\mu$ M of BldDN (bottom left). The signals of free probes and probes complexed with BldD or BldDN were indicated by arrows. Dissociation constants ( $K_D$ ) of BldD (top right) and BldDN (bottom right) were determined by plotting percent of BldD or BldDN bound to *pblidD* against the logarithm of concentrations of BldD or BldDN used (see *Experimental procedures*):  $K_D$  (BldD) = 0.529 ( $\pm 0.004$ )  $\mu$ M;  $K_D$  (BldDN) = 1.159 ( $\pm 0.02$ )  $\mu$ M.

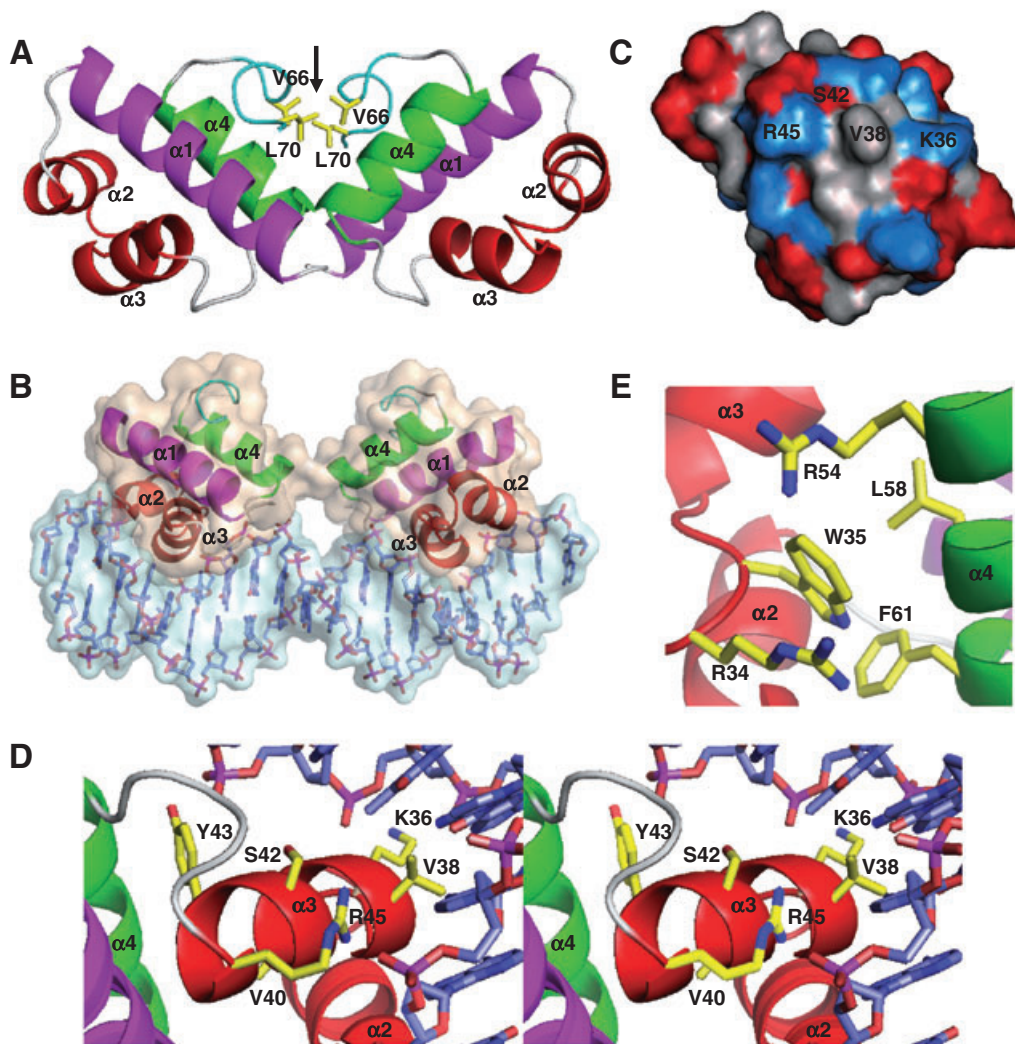


**Fig. 4.** Dimerization and BldDN/DNA complex model.

A. A ribbon representation of BldDN dimer observed in the crystal packing shown with the secondary structures labelled. Val66 and Leu70 that are involved in the dimerization of BldDN are labelled and indicated by arrow.

B. Model of BldDN/DNA complex represented with molecular surface. The BldDN structure was superimposed onto the lambdaDN/DNA complex structure, and then refined to remove steric conflicts.

C. Surface representation of BldDN. The exposed surface is coloured based on the underlying atoms: grey, all hydrophobic residues (Ala, Gly, Val, Leu, Ile, Pro, Phe, Tyr, Trp and Met); red, all non-charged polar and negative charged residues (Asn, Gln, Ser, Thr, Cys, Asp and Glu); blue, all positive charged residues (Arg, Lys and His). The orientation is similar to Fig. 1A.

D. Stereo view of the BldDN–DNA contacts in BldDN/DNA model with the secondary structure and important residues labelled.

E. A ribbon diagram drawing the interactions between residues of turn23 and  $\alpha 4$ .

repressor follows this rule faithfully. However, interestingly, the 'turn' connecting  $\alpha 2$  and  $\alpha 3$  of BldDN is composed of four residues although it starts from glycine (Fig. 2). This is of particular interest because BldD binds to multiple operator sites containing an asymmetric inverted repeat with limited sequence conservation, that is, various conformations would be required for BldD dimer to specifically recognize them. Considering that the 'turn' region is involved in maintaining relative orientation and distance between  $\alpha 2$  and  $\alpha 3$  for the stable protein–DNA complex, a longer 'turn' could allow additional flexibility for BldD to

recognize and regulate more target genes than the lambda repressor. In addition, the selective defects observed in R34A, W35A and R34A/W35A mutants suggest that turn23 of BldD also contributes to the specific recognition of multiple operator sites like Ser42.

#### *Construction of a bldD null mutant and in vivo complementation experiments*

In order to investigate the role of  $\alpha 3$  and turn23 *in vivo*, we constructed a *bldD* null mutant (Fig. 6A–C) (see

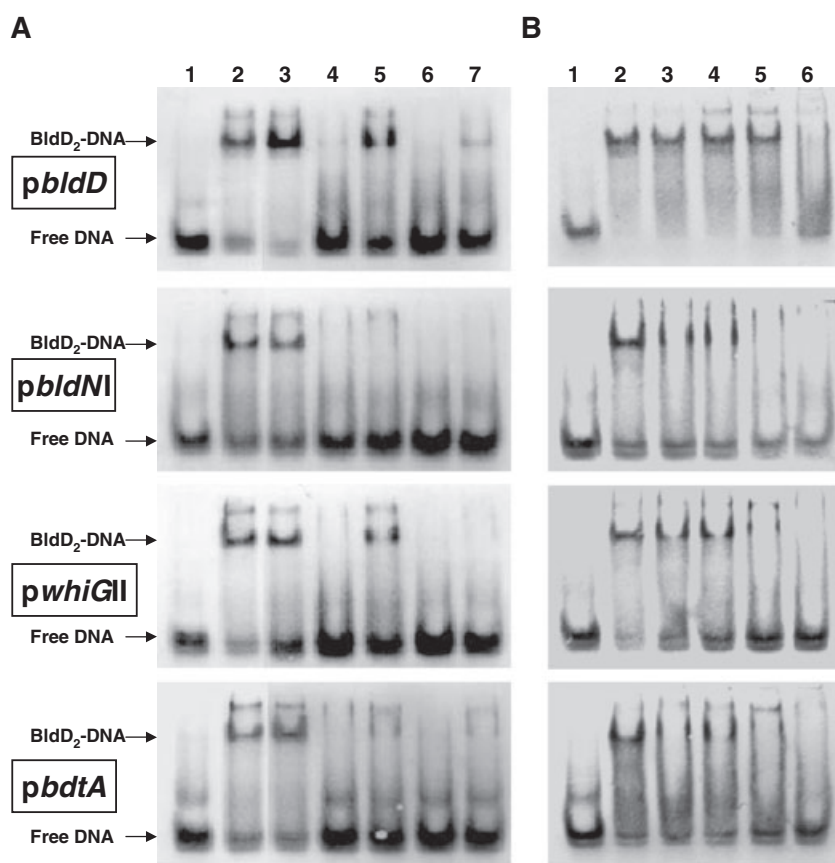


**Fig. 5.**  $\alpha 3$  and turn23 are important for DNA binding of full-length BldD. His-tagged full-length BldD and nine mutants possessing a single mutation at  $\alpha 3$  (A) and turn23 (B) were used for EMSA experiments against four BldD-binding sites: *pblbD*, *pblbNI*, *pwhiGII* and *pbdtA*. The free probe and probe complexed with BldD are indicated by arrows. Two micrograms of BldD and BldD mutant proteins were mixed with each probe and loaded onto 10% native gel containing 1 $\times$  TBE.

A. Lane 1, free probe; lane 2, wild type; lane 3, V38A; lane 4, V40A; lane 5, S42A; lane 6, Y43A; lane 7, R45A.

B. Lane 1, free probe; lane 2, wild type; lane 3, R34A; lane 4, W35A; lane 5, R34A/W35A; lane 6, K36A.

*Experimental procedures*) and tested whether BldD point mutants used in this study could complement aerial mycelium formation of the *bldD* mutant. For this purpose, we introduced pSET162 (see *Experimental procedures*) derivatives containing wild-type *bldD* and *bldD* with point mutations into the *bldD* null mutant.

As shown in Fig. 6D and E, K36A, V40A, Y43A and R45A mutants, which exhibited almost complete loss of DNA-binding activity in EMSA experiment, failed to complement the *bld* phenotype. W35A, R34A/W35A and S42A mutants, which selectively bound to BldD-target promoters *in vitro*, showed slightly retarded the formation of aerial mycelia compared with wild-type BldD (Fig. 6D and E). It is likely that the ability of these mutants to bind to BldD-target promoters, despite its selectivity and low affinity, still can make the development proceed. Why R34A showed most severe defect compared with W35A, R34A/W35A and S42A (Fig. 6E) is unclear. However, these results together with the EMSA data suggest that Ser42 and turn23 are involved in the recognition of multiple promoters with low sequence conservation.

#### Cooperative binding of BldD

Elliot *et al.* (2001) demonstrated BldD binds to two oper-

ator sites in each promoter region of *bldN* (*pblbNI* and *pblbMII*) and *whiG* (*pwhiGI* and *pwhiGII*) respectively. As the quantity of BldD was increased, three differently retarded bands showed rapid transition into the most retarded species. Furthermore, it was reported that BldD exists as a mixture of dimers and tetramers in solution with the ratio of 7:2, indicating that BldD could form a tetramer in certain environments (Elliot *et al.*, 2003). These results, together with the fact that the structure of BldDN is highly homologous to that of lamdaN whose repression activity is achieved by the cooperative binding, suggest the cooperativity between BldD proteins on DNA binding.

To test this hypothesis, the DNA-binding activity of full-length BldD against the operator sites of *bldN* and *whiG* were investigated. Because BldD binds to the promoter region of *bldD* as a dimer (Elliot *et al.*, 2003) and all the DNA probes used in our EMSA experiments have similar lengths about 30 bp containing one inverted repeat (see *Experimental procedures*), we can safely assume that the retarded bands in Fig. 7 are a BldD<sub>2</sub>-DNA complex. Interestingly, BldD binds to the *pblbNI* (from -29 to -2) with high affinity and exhibits nearly negligible affinity to the *pblbMII* (from +33 to +59) (Fig. 7A). Similarly, BldD exhibits its DNA-binding affinity only to the *pwhiGII*, not to *pwhiGI*

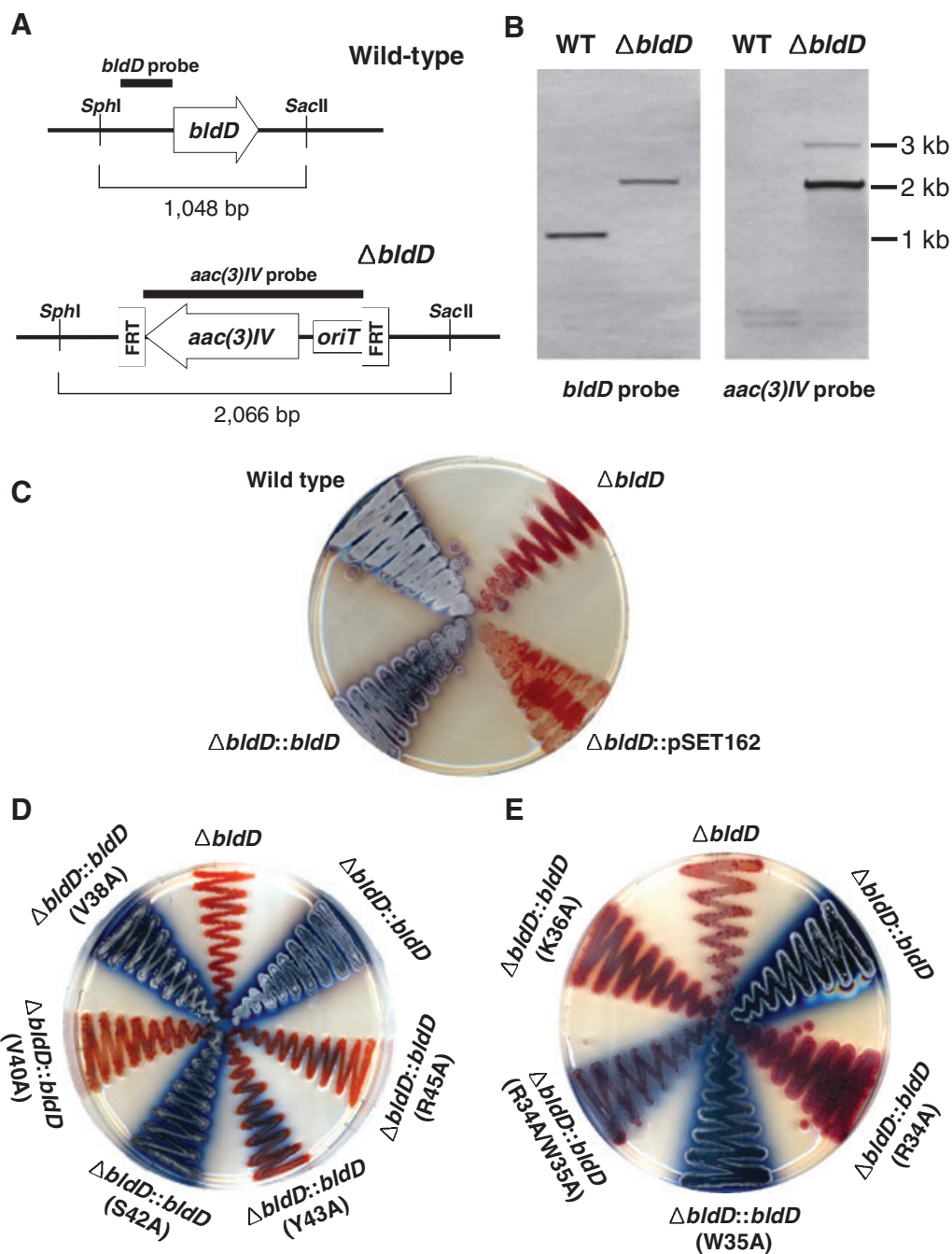


**Fig. 6.** Construction of a *bldD* null mutant and *in vivo* complementation experiment.

A. Schematic diagram of the chromosomal DNA of wild-type and disrupted *bldD* showing the location of the *SphI* and *SacII* sites and the sizes of the resulting digestion products. FRT, flip recombinase target; *aac(3)IV*, apramycin resistance gene; *oriT*, origin of transfer. The location of each probe used for southern analysis is indicated by thick bar.

B. Genomic southern analysis confirming *bldD* deletion and replacement by *aac(3)IV*. Two micrograms of total genomic DNA were digested with *SphI* and *SacII*, separated on a 1% agarose gel, transferred to nylon membrane (Amersham Biosciences), and hybridized with Dig-labelled *bldD* probe (left) and *aac(3)IV* probe (right). The sizes of DNA marker bands are shown on the right. WT indicates wild-type *S. coelicolor*.

C. Phenotype of the constructed *bldD* null mutant strain. The  $\Delta bldD$  strain showed *bld* phenotype as described by Elliot *et al.* (2003). The *bld* phenotype of  $\Delta bldD$  strain was restored by introduction of pSET162 plasmid containing wild-type *bldD* gene into the  $\Delta bldD$  strain. pSET162 was used as a negative control.

D. Phenotype of the  $\Delta bldD$  strain complemented by introduction of pSET162 derivatives containing wild-type *bldD* and *bldD* with point mutations on  $\alpha 3$ .

E. Phenotype of the  $\Delta bldD$  strain complemented by introduction of pSET162 derivatives containing wild-type *bldD* and *bldD* with point mutations on turn23.

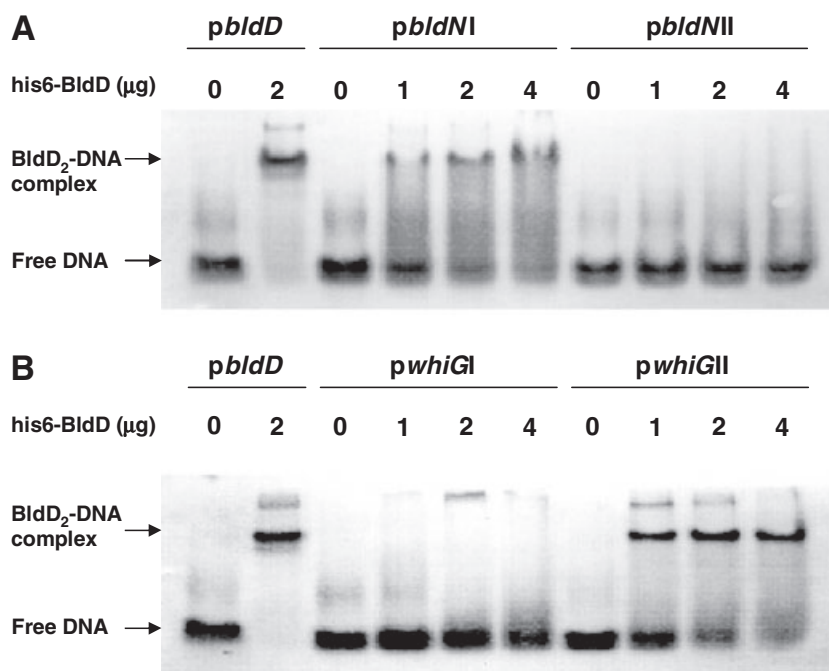


**Fig. 7.** Selective binding of BldD against two operator sites of *bldN* (A) and *whiG* (B). Different amount of wild-type BldD protein was mixed with each probe and loaded onto 10% native gel. The separated products, free DNA and BldD-bound DNA, are indicated by arrows. Because BldD binds to its own promoter (*pblD*) as a dimer, we regard the shifted bands in A and B as a BldD<sub>2</sub>-DNA complex.

(from -25 to +2) (Fig. 7B). The selective DNA-binding activity of BldD toward separated operator sites and the fact that BldD binds to two operator sites, when they are connected, indicate that the binding of one BldD dimer to *pblDM* site could cooperatively facilitate the binding of the second BldD dimer to *pblDMI*.

The two operator sites of *bldN* and *whiG* are separated by 9.8 turn (103 bp) and 5.8 turn (61 bp), respectively, as assuming 10.5 bp per turn. One possible model for the cooperative binding to two operator sites far away from each other is the binding of BldD dimers through DNA bending like lambda repressor. When lambda repressor and DNA were incubated under the conditions for cooperative binding, repressors at the separated sites touch each other and the DNA bends smoothly in order to accommodate the protein-protein interaction (Griffith *et al.*, 1986; Hochschild and Ptashne, 1986).

#### Mutational analysis of Tyr62 residue

*BldD* mutant allele was first identified as an A(r)G point mutation changing a tyrosine residue at position 62 to a cysteine (Y62C) (Elliot *et al.*, 1998). Elliot *et al.* (2003) reported that the Y62C point mutation has the same effect as the whole deletion of *bldD* gene, implying that Tyr62 plays a critical role in either the function or the stability of the protein.

In order to verify the role of Tyr62 in BldD, Tyr62 was substituted with Cys, Ser and Phe respectively. As shown in Fig. 8B, Y62F mutant remained soluble, whereas two mutants Y62C and Y62S exhibits highly reduced solubility

(almost all proteins went into the insoluble fraction). This result can be explained by the role of Tyr62 in stabilizing the BldDN structure. The side chain of Tyr62 aims toward the centre of the globular domain of BldDN and is thus extensively implicated in the formation of a hydrophobic core together with Leu13, Val27, Trp35, Val40, Leu58 and Phe61 (Fig. 1B). In addition, Tyr62 forms a T-shaped aromatic-aromatic interaction with the adjacent Phe61 stabilizing the C-terminus end of  $\alpha 4$  by helix capping (Burley and Petsko, 1985) (Figs 1B and 8A). Therefore, substitution of Tyr62 with small residues such as Cys and Ser would disrupt the hydrophobic core and destabilize  $\alpha 4$ . Consistently Y62F mutant was able to complement the *bldD* null mutant, while Y62C and Y62S mutants failed (Fig. 8C).

Several lines of evidences have suggested that aromatic residues contribute to the stability of proteins when they occupy the interior of proteins for hydrophobic interactions (Serrano *et al.*, 1991; Sekharudu *et al.*, 1992; Anderson *et al.*, 1993; Nam *et al.*, 2001). For example, mutation of Tyr55, in the active-site cavity of ketosteroid isomerase (KSI) from *Pseudomonas putida*, to Ser resulted in a decrease of stability by about 9.5 kcal mol<sup>-1</sup> and disrupted the helical structure of Tyr55-containing helix, suggesting that the aromatic side chain of the tyrosine residue contributes to conformational stability of KSI (Nam *et al.*, 2001). In fact, Y62F mutant retains its solubility (Fig. 8B), indicating that the aromatic-aromatic interaction between Phe62 and Phe61 still stabilizes  $\alpha 4$  and hydrophobic core. As a conclusion, because the Y62C mutation disrupts the

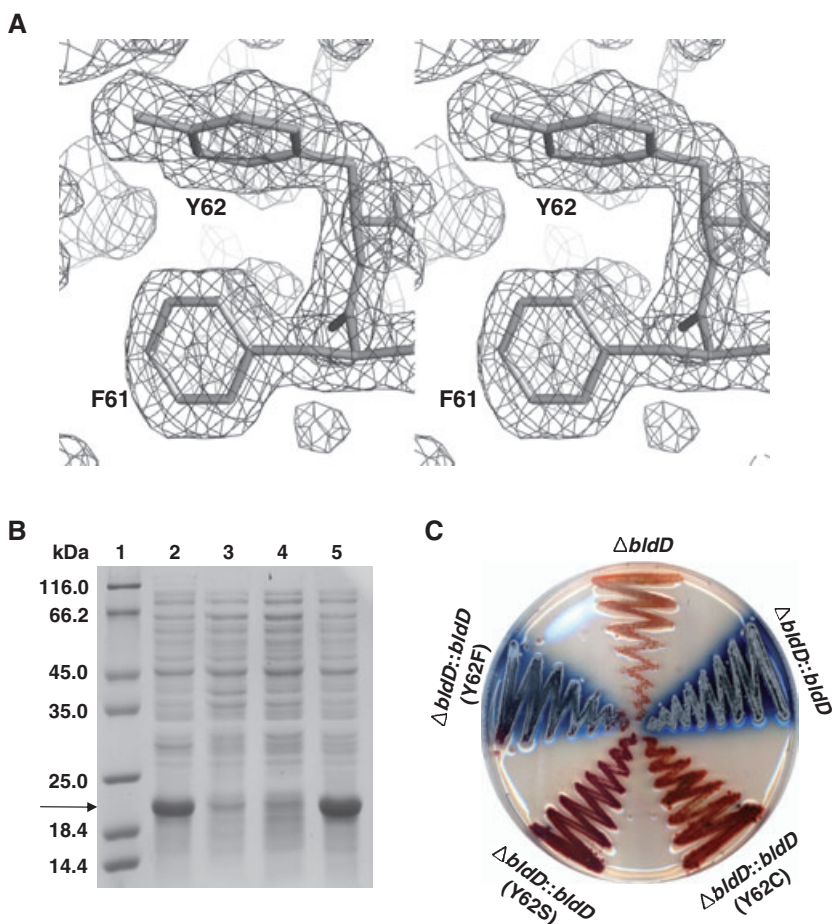


**Fig. 8.** The role of Tyr62 in the hydrophobic core formation.

A. The  $2F_o - F_c$  electron density map contoured at  $1\sigma$  showing the T-shaped aromatic-aromatic interaction between Phe61 and Tyr62 of BldDN at 1.8 Å.

B. Mutational analysis of Tyr62 residue. His-tagged full-length BldD and three mutants possessing a single mutation at Tyr62 were expressed in *E. coli*. The black arrow indicates the position of his6-BldD. Twenty-five micrograms of crude extracts were loaded onto 12% SDS-PAGE. Lane 1, marker; lane 2, wild type; lane 3, Y62C; lane 4, Y62S; lane 5, Y62F.

C. Phenotype of the  $\Delta bldD$  strain complemented by introduction of pSET162 derivatives containing wild-type *bldD* and three mutants with a single mutation at Tyr62.

hydrophobic core, the Y62C mutant is destabilized and thus loses its function.

#### Feasible mechanism for the regulation of BldD activity

Upon the initiation of aerial hyphae formation in *S. coelicolor*, the transcription of *bldN* that is essential for the erection of aerial hyphae is significantly derepressed (Elliot *et al.*, 2001). This result suggests that the repressor activity of BldD against *bldN* should be overcome for aerial hyphae formation. Elliot *et al.* (1998) proposed a phosphorylation at Tyr62 for this derepression mechanism, because the only known *bldD* mutant allele except for the *bldD*-deleted mutant has an Y62C point mutation. However, our structure clearly reveals that Tyr62 is placed inside of BldDN (solvent accessible surface area for the OH of Tyr62 is 0 Å<sup>2</sup>), and thus is crucial for the hydrophobic core formation (Figs 1B and 8A). Therefore, it is unlikely that the regulation of BldD activity is mediated by phosphorylation at Tyr62.

The fact that BldDN structure is closely related to the XRE-family of transcription factors provides us two feasible derepression mechanisms. First, BldD activity could be regulated by proteolytic cleavage like lambda repres-

or. In lambda repressor, the repressor activity is regulated by *Escherichia coli* RecA-mediated self-cleavage between N- and C-terminal domains (Roberts and Roberts, 1975; Kim and Little, 1993). However, because BldD has no self-cleavage site, it could be cleaved or degraded by a certain stage-specific protease. Second, the derepression could be achieved by BldD-sequestering like SinR. SinI blocks the repressor activity of SinR by sequestering the SinR as a heterodimer (Bai *et al.*, 1993; Lewis *et al.*, 1998). Further analysis about whether BldD is cleaved or sequestered and, if it is, which protein is involved in this process is a great challenge in the future.

In summary, we determined the crystal structure of the DNA-binding domain of BldD, and could identify putative residues required for DNA recognition from the structural, mutational and *in vivo* complementational analyses: Lys36, Tyr43 and Arg45 play a critical role in DNA binding, and Arg34, Trp35 and Ser42 appear to be involved in the specific recognition of multiple promoters. The molecular basis for the loss of protein activity of the Y62C mutant was also suggested based on the role of Tyr62 for the hydrophobic core formation. In addition, our biochemical assay supports the possibility of cooperative binding of BldD to its target sites. Our future studies will be focused

on the verification of the mechanism for relief from the repressor activity of BldD and the identification of proteins involved in this process.

## Experimental procedures

### Bacterial strains and growth conditions

For overexpression and selenomethionine-labelling, *E. coli* strain BL21 (ED3) and B834 (DE3) (Novagen) were used respectively. *E. coli* BW25113 (Datsenko and Wanner, 2000) was used to propagate the recombination plasmid pIJ790 and *S. coelicolor* cosmids. *E. coli* ET12567/pUZ8002 (Paget *et al.*, 1999) was the non-methylating plasmid donor strain during conjugal gene transfer from *E. coli* to *Streptomyces*. *E. coli* strains were grown in Luria–Bertani medium at 37°C, and *S. coelicolor* A3(2) was cultured on R2YE and MS agar (Kieser *et al.*, 2000) at 30°C. Ampicillin (Sigma) and thiostrpton (Sigma) were used at 100 and 30 µg ml<sup>-1</sup>, and kanamycin (Sigma) and apramycin (Sigma) were used at 50 µg ml<sup>-1</sup>.

### Protein purification, crystallization and structure determination

BldDN from *S. coelicolor* A3(2) was expressed in *E. coli* and purified as described previously (Kim *et al.*, 2004). Because BldDN contains no methionine residue except for the N-terminal methionine, one glutamine residue (Gln20) was mutated to methionine (Q20M) (Kim *et al.*, 2004) to ensure an anomalous signal in the X-ray diffraction experiment. Gln20 residue was selected on the basis of a secondary structure prediction using Jpred server (Cuff *et al.*, 1998), which suggested that this residue might be located at the terminus of  $\alpha$ -helix region. For the selenomethionine labelling

of BldDN-Q20M mutant, methionine auxotroph *E. coli* B834 (DE3) (Novagen) strain was used as a host for plasmid transformation. The selenomethionyl BldDN-Q20M mutant protein was purified by an identical procedure to that for the wild-type BldDN. The purified SeMet BldDN-Q20M was concentrated to approximately 10 mg ml<sup>-1</sup> for crystallization.

Native BldDN crystals (C2;  $a = 77.2$ ,  $b = 31.8$  and  $c = 33.6$  Å,  $\beta = 105.1^\circ$ , a monomer in asymmetric unit) were grown and a 1.8 Å data set was obtained with a Macscience 2030b imaging plate at Beamline 6B at Pohang Light Source as described previously (Kim *et al.*, 2004).

The selenomethionyl BldDN-Q20M crystals were grown as described previously (Kim *et al.*, 2004). These crystals belonged to space group P2<sub>1</sub> with cell parameters  $a = 33.7$ ,  $b = 70.5$  and  $c = 38.8$  Å,  $\beta = 112.3^\circ$ , and contained two monomers per asymmetric unit. Diffraction data were processed and scaled with programs DENZO and SCALEPACK from the HKL program suite (Otwinowski and Minor, 1997). The structure was solved by the multi-wavelength anomalous dispersion (MAD) method using three wavelength data sets of the selenomethionyl Q20M mutant crystal: the peak wavelength was at 0.97932 Å, and the inflection wavelength was at 0.97942 Å, and the remote wavelength was at 0.98722 Å. Three selenium sites were located, and phase refinement was carried out by using the programs SOLVE and RESOLVE (Terwilliger, 1999; Terwilliger and Berendzen, 1999). Initial phasing and model building was performed with Q20M MAD data set. Model building was performed using the program QUANTA software (Molecular Simulations) and refined with CNS (Brunger *et al.*, 1998) to an  $R_{\text{free}}$  of 0.268 and  $R_{\text{work}}$  of 0.252 in the resolution range of 20–2.3 Å. The native BldDN structure was solved by molecular replacement with CNS using the Q20M structure as a search model, and refined to  $R_{\text{free}}$  of 0.225 and  $R_{\text{work}}$  of 0.188 in the resolution range of 20–1.8 Å. The refinement statistics for the native BldDN structure are summarized in Table 1. The ideality of the model stere-

**Table 1.** Summary of crystallographic analysis.

Data sets, space group	Q20M selenium data (space group: P2 <sub>1</sub> )			Native BldDN (space group: C2)
	Peak	Inflection	Remote	
Wavelength (Å)	0.97932	0.97942	0.98722	1.12714
Resolution (Å)	20–2.3	20–2.3	20–2.3	20–1.8
Completeness (%) <sup>a</sup>	97.8 (99.7)	97.0 (98.8)	95.8 (97.8)	96.7 (94.9)
$R_{\text{sym}}$ (%) <sup>a,b</sup>	3.9 (5.9)	3.3 (5.6)	3.2 (5.2)	3.1 (7.1)
Average $I/\sigma$	28.8 (20.9)	28.7 (21.5)	25.6 (19.8)	29.7 (21.0)
Refinement statistics				
Resolution range (Å)				20–1.8
Number of reflections	14134	14230	13930	17663
Total number of atoms				
Total				713
Water				147
Completeness of data (%)				96.7
$R^2$ ( $R_{\text{free}}$ ) (%)				18.8 (22.5)
r.m.s. deviations <sup>d</sup>				
Bonds (Å)				0.004
Angles (°)				0.954

a. The number in parentheses is for the outer shell.

b.  $R_{\text{sym}} = \sum_h \sum_i |I_{h,i} - I_h| / \sum_h \sum_i I_{h,i}$ , where  $I_h$  is the mean intensity of the  $i$  observations of symmetry related reflections of  $h$ .

c.  $R = \sum |F_o - F_c| / \sum F_o$ , where  $F_o = F_p$ , and  $F_c$  is the calculated protein structure factor from the atomic model.  $R_{\text{free}}$  was calculated with 10% of the reflections.

d. Root mean square (r.m.s) deviations in bond length and angles are the deviations from ideal values.

ochemistry was verified by PROCHECK (Laskowski *et al.*, 1993). The Ramachandran plots indicate 95.1% of non-glycine residues are in the most favoured regions, and all others are in the additionally allowed regions.

#### Determination of oligomeric state of BldDN

Purified recombinant BldDN and low molecular mass standards (Amersham Biosciences) were applied on a Superdex 75 16/60 column (Amersham Biosciences) pre-equilibrated with 20 mM Tris-HCl (pH 8.0) containing 150 mM NaCl. A standard curve was generated by plotting the logarithm of molecular mass of standard proteins against their  $K_{av}$ , where  $K_{av} = (V_e - V_o)/(V_t - V_o)$ :  $V_e$ , elution volume;  $V_o$ , void volume;  $V_t$ , total bed volume.  $K_{av}$  of BldDN determined by using the same column was compared with the profile of protein standards: bovine serum albumin (67 kDa), ovalbumin (43 kDa), chymotrypsinogen A (25 kDa) and ribonuclease A (13.7 kDa).

#### Site-directed mutagenesis of BldD

For site-directed mutagenesis of the full-length BldD proteins, the gene encoding the full-length BldD was amplified by polymerase chain reaction (PCR) using *S. coelicolor* A3(2) genomic DNA as a template. The PCR product was digested with NdeI and BamHI and inserted downstream of the T7 promoter of the pET-15b (Novagen) generating pET-15b-BldD. The Quickchange site-directed mutagenesis kit (Stratagene) was used with a template of pET-15b-BldD and proper primer pairs for each mutation. The mutations were confirmed by sequencing the purified plasmids.

#### Purification of BldD and its mutants

For overexpression and purification of full-length BldD proteins, pET-15b-BldD plasmid was transformed into *E. coli* strain BL21 (DE3). His-tagged BldD (his6-BldD) was purified by an identical procedure to that for the BldDN except for the thrombin treatment and concentrated to approximately 1 mg ml<sup>-1</sup>.

BldD mutants generated from the site-directed mutagenesis were overexpressed and purified by an identical procedure to that for the his6-BldD and also concentrated to approximately 1 mg ml<sup>-1</sup>.

#### Electrophoretic mobility shift assay

To prepare DNA probes for EMSA, complementary oligonucleotides were synthesized as bellow.

pwhiGI-F AAGGTGTTTCGAGTGATCACCCAGAGCGA  
 pwhiGI-R ATCGCTCTGGGTGATCACTCGAACACCT  
 pwhiGII-F AAGTCCAGTCACGCTACGCTCACGATGA  
 pwhiGII-R ATCATCGTGAGCGTAGCGTGACTGGACT  
 pbldNI-F ACAGTGCCTGCACGAAGCGTTATTCTCCT  
 pbldNI-R AAGGAGAATAACGCTTTCGTGCAGGCACTG  
 pbldNII-F ACGGGTGAATGGTTCCGTACTGCACGTG  
 pbldNII-R ACACGTGCAGTACGGAACCATTACCCG

pbdtA-F AGCACGCAGCGACGAAGAGTCACCGGAA  
 pbdtA-R ATTCCGGTGACTCTTCGTGCGCTGCGTGC  
 pbldD-F AAGCAGAGTAACGCTGCGTAACCTCACA  
 pbldD-R ATGTGAGGTTACGCAGCGTTACTCTGT

These oligonucleotides were annealed in an annealing buffer containing 20 mM Tris-HCl (pH 7.5), 10 mM MgCl<sub>2</sub> and 50 mM NaCl. The annealing mixture was heated to 100°C for 10 min and then slowly cooled to 30°C. These annealed oligonucleotides were end-labelled by Klenow fragment with dig-dUTP (Roche) for 1 h and used for EMSA experiments.

EMSA were performed using the dig-labelled probes. BldD and BldD mutants were incubated with dig-labelled probes at 30°C for 20 min in a buffer containing 10 mM Tris-HCl (pH 7.8), 150 mM NaCl, 2 mM dithiothreitol, 1 µg of poly dI-dC, and 10% glycerol. The DNA-protein complexes were run out on 10% native polyacrylamide gel. The gel was transferred to Nylon membrane and colour development was performed with addition of nitroblue tetrazolium and 5-bromo-4-chloro-3-indolyl phosphate following the manufacturer's instructions.

#### Determination of the dissociation constant ( $K_D$ ) of BldD and BldDN

Electrophoretic mobility shift experiments using DIG-labelled *pbldD* with 0.15–1.5 µM of BldD or 0.3–3.0 µM of BldDN were performed and the developed bands were quantified by using LAS-3000 (FUJIFILM) and Multi Gauge V3.0 software. Band intensities for the DNA-protein complexes were reported as percentage of total signals plotted against the logarithm of protein concentration. Binding constant,  $K_D$ , was determined using the Hill's equation,  $\log(T-Y)/(Y-B) = h(\log[S] - \log K_D)$ , where  $[S]$  is protein concentration,  $h$  is Hill's coefficient,  $Y$  is signal intensities of protein-DNA complexes,  $T$  and  $B$  are maximum and minimum signals of protein-DNA complexes. All data were analysed by using GraphPad Prism version 4.0.

#### Construction of a *bldD* null mutant

The chromosomal *bldD* gene of *S. coelicolor* A3(2) was disrupted using the REDIRECT® technology (Plant Bioscience) (Gust *et al.*, 2003). The disruption cassette was prepared by same procedure as described by Elliot *et al.* (2003). Briefly, a disruption cassette containing *oriT* and the *aac(3)IV* gene (apramycin resistance marker) was prepared using pIJ773 as a template and primers (CGA17 and CGA16) that have 39 nucleotide extensions specific for the upstream and downstream of the start and stop codon of *bldD* open reading frame (ORF) (Elliot *et al.*, 2003) and then, this PCR-amplified disruption cassette was introduced by electroporation into *E. coli* BW25113 bearing the *bldD* cosmid, SC9C5 (provided by H. Kieser, John Innes Centre) and pIJ790 for λRED-mediated high frequency recombination between the disruption cassette and the SC9C5 cosmid. Finally, unmethylated PCR-targeted cosmid DNA that is prepared using the methylation-deficient *E. coli* strain ET12567/pUZ8002 was introduced by bacterial conjugation into *S. coelicolor* A3(2) to allow replacement of the *aac(3)IV* gene with the chromosomal *bldD* gene. Despite low efficiency of generating exoconjugants displayed

as an apramycin<sup>R</sup> and kanamycin<sup>S</sup> phenotype, correct *bldD* mutant as a result of double-crossover between the *aac(3)IV* and the chromosomal *bldD* gene was acquired. To confirm *bldD* deletion mutant, chromosomal DNA from wild type and *bldD* deletion mutant were digested with SphI and SacII and subjected to Southern analysis with either a PCR-amplified, DIG-labelled DNA fragment of upstream region of *bldD* ORF (encompassing from -236 to -26 nucleotides relative to translation start site), or a PCR-amplified, DIG-labelled DNA fragment from *aac(3)IV* and *oriT* region of pJ773 as a probe (Fig. 6A and B).

#### In vivo complementation experiment

In order to construct a complementation plasmid for wild-type *bldD*, DNA fragments containing promoter and ORF of *bldD* were amplified by PCR and cloned into pGEM-Teasy (Promega) generating pGEMT::P*bldD*-*bldD*. Fragment (0.75 kb) of pGEMT::P*bldD*-*bldD* was ligated into pSET162 which is made by insertion of a thiostrepton resistance marker at SphI site of pSET152 (Bierman *et al.*, 1992), generating pSET::P*bldD*-*bldD*. To construct complementation plasmids for BldD point mutants, 0.75 kb BamHI-EcoRI fragment of pSET::P*bldD*-*bldD* was cloned into pGEX-4T-1 (Amersham biosciences) generating pGEX::P*bldD*-*bldD*. and then, 0.5 kb NdeI-BamHI fragments of pET-15b-BldD possessing *bldD* point mutations were exchanged with *bldD* in pGEX::P*bldD*-*bldD*. Finally, the 0.75 kb EcoRI-BamHI fragments of pGEX::P*bldD*-*bldD* harbouring point mutations were moved to pSET162. The reintegration constructs were verified by sequencing the purified pSET162 series.

The complementation constructs (pSET162 derivatives) were introduced into methylation negative, conjugal host strain ET12567/pUZ8002 and were integrated into the chromosomal DNA of the *bldD* deletion mutant by bacterial conjugation. The proper integration exoconjugants showing the apramycin<sup>R</sup> and thiostrepton<sup>R</sup> phenotype were verified by genomic PCR analysis using their chromosomal DNA as a template. For phenotypic analysis, strains harbouring point mutations on *bldD* were plated on solid R2YE media at 30°C and cell growth were monitored over a 5 day period.

#### Coordinates

Coordinate has been deposited in the Protein Data Bank with Accession number 2EWT.

#### Acknowledgements

We thank Dr Keith F. Chater and John Innes Centre for providing us general and genetic backgrounds of *Streptomyces coelicolor* A3(2), Plant Bioscience for the gift of the REDIRECT constructs and strains. Work performed at Seoul National University was supported by a Korea Science and Engineering Foundation (KOSEF) Grant (R01-2004-000-10264) and by a research fellowship of the BK21 project and work performed at Pohang Accelerator Laboratory was supported by a grant from the Biogreen 21 Program (20050301034479), Rural Development Administration, Republic of Korea.

#### References

- Anderson, D.E., Hurley, J.H., Nicholson, H., Baase, W.A., and Matthews, B.W. (1993) Hydrophobic core repacking and aromatic-aromatic interaction in the thermostable mutant of T4 lysozyme Ser 117→Phe. *Protein Sci* **2**: 1285–1290.
- Bai, U., Mandic-Mulec, I., and Smith, I. (1993) SinI modulates the activity of SinR, a developmental switch protein of *Bacillus subtilis*, by protein–protein interaction. *Genes Dev* **7**: 139–148.
- Bateman, A., Birney, E., Durbin, R., Eddy, S.R., Finn, R.D., and Sonnhammer, E.L. (1999) Pfam 3.1:1313 multiple alignments and profile HMMs match the majority of proteins. *Nucl Acids Res* **27**: 260–262.
- Beamer, L.J., and Pabo, C.O. (1992) Refined 1.8 Å crystal structure of the lambda repressor–operator complex. *J Mol Biol* **227**: 177–196.
- Bell, C.E., and Lewis, M. (2001) Crystal structure of the lambda repressor C-terminal domain octamer. *J Mol Biol* **314**: 1127–1136.
- Bibb, M.J., Molle, V., and Buttner, M.J. (2000)  $\sigma^{BldD}$ , an extra-cytoplasmic function RNA polymerase sigma factor required for aerial mycelium formation in *Streptomyces coelicolor* A3(2). *J Bacteriol* **182**: 4606–4616.
- Bierman, M., Logan, R., O'Brien, K., Seno, E.T., Rao, R.N., and Schoner, B.E. (1992) Plasmid cloning vectors for the conjugal transfer of DNA from *Escherichia coli* to *Streptomyces* spp. *Gene* **11**: 43–49.
- Brennan, R.G., and Matthews, B.W. (1989) The helix-turn-helix DNA binding motif. *J Biol Chem* **264**: 1903–1906.
- Brunger, A.T., Adams, P.D., Clore, G.M., DeLano, W.L., Gros, P., Grosse-Kunstleve, R.W., *et al.* (1998) Crystallography & NMR system: a new software suite for macromolecular structure determination. *Acta Crystallogr Sect D Biol Crystallogr* **54**: 905–921.
- Burley, S.K., and Petsko, G.A. (1985) Aromatic–aromatic interaction: a mechanism of protein structure stabilization. *Science* **229**: 23–28.
- Champness, W.C. (1988) New loci required for *Streptomyces coelicolor* morphological and physiological differentiation. *J Bacteriol* **170**: 1168–1174.
- Chater, K.F. (1972) A morphological and genetic mapping study of white colony mutants of *Streptomyces coelicolor*. *J General Microbiol* **72**: 9–28.
- Chater, K.F. (1993) Genetics of differentiation in *Streptomyces*. *Annu Rev Microbiol* **47**: 685–713.
- Chater, K.F. (1998) Taking a genetic scalpel to the *Streptomyces* colony. *Microbiology* **144**: 1465–1478.
- Chater, K.F., Bruton, C.J., Plaskitt, K.A., Buttner, M.J., Mendez, C., and Helmann, J.D. (1989) The developmental fate of *S. coelicolor* hyphae depends upon a gene product homologous with the motility sigma factor of *B. subtilis*. *Cell* **59**: 133–143.
- Cuff, J.A., Clamp, M.E., Siddiqui, A.S., Finlay, M., and Barton, G.J. (1998) JPred: a consensus secondary structure prediction server. *Bioinformatics* **14**: 892–893.
- Datsenko, K.A., and Wanner, B.L. (2000) One-step inactivation of chromosomal genes in *Escherichia coli* K-12 using PCR products. *Proc Natl Acad Sci USA* **97**: 6640–6645.
- Elliot, M.A., and Leski, B.K. (1999) The BldD protein from

- Streptomyces coelicolor* is a DNA-binding protein. *J Bacteriol* **181**: 6832–6835.
- Elliot, M., Damji, F., Passantino, R., Chater, K., and Leskiw, B. (1998) The *blbD* gene of *Streptomyces coelicolor* A3(2): a regulatory gene involved in morphogenesis and antibiotic production. *J Bacteriol* **180**: 1549–1555.
- Elliot, M.A., Bibb, M.J., Buttner, M.J., and Leskiw, B.K. (2001) BldD is a direct regulator of key developmental genes in *Streptomyces coelicolor* A3(2). *Mol Microbiol* **40**: 257–269.
- Elliot, M.A., Locke, T.R., Galibois, C.M., and Leskiw, B.K. (2003) BldD from *Streptomyces coelicolor* is a non-essential global regulator that binds its own promoter as a dimer. *FEMS Microbiol Lett* **225**: 35–40.
- Gaur, N.K., Dubnau, E., and Smith, I. (1986) Characterization of a cloned *Bacillus subtilis* gene that inhibits sporulation in multiple copies. *J Bacteriol* **168**: 860–869.
- Griffith, J., Hochschild, A., and Ptashne, M. (1986) DNA loops induced by cooperative binding of lambda repressor. *Nature* **322**: 750–752.
- Gust, B., Challis, G.L., Fowler, K., Kieser, T., and Chater, K.F. (2003) PCR-targeted *Streptomyces* gene replacement identifies a protein domain needed for biosynthesis of the sesquiterpene soil odor geosmin. *Proc Natl Acad Sci USA* **100**: 1541–1546.
- Harrison, S.C., and Aggarwal, A.K. (1990) DNA recognition by proteins with the helix-turn-helix motif. *Annu Rev Biochem* **59**: 933–969.
- Hochschild, A., and Ptashne, M. (1986) Homologous interactions of lambda repressor and lambda Cro with the lambda operator. *Cell* **44**: 925–933.
- Hodgson, D.A. (2000) Primary metabolism and its control in streptomycetes: a most unusual group of bacteria. *Adv Microb Physiol* **42**: 47–238.
- Holm, L., and Sander, C. (1997) Dali/FSSP classification of three-dimensional protein folds. *Nucl Acids Res* **25**: 231–234.
- Jordan, S.R., and Pabo, C.O. (1988) Structure of the lambda complex at 2.5 Å resolution: details of the repressor-operator interactions. *Science* **242**: 893–899.
- Keijsers, B.J., van Wezel, G.P., Canters, G.W., and Vijgenboom, E. (2002) Developmental regulation of the *Streptomyces lividans* *ram* genes: involvement of RamR in regulation of the *ramCSAB* operon. *J Bacteriol* **184**: 4420–4429.
- Kelemen, G.H., and Buttner, M.J. (1998) Initiation of aerial mycelium formation in *Streptomyces*. *Curr Opin Microbiol* **1**: 656–662.
- Kelemen, G.H., Viollier, P.H., Tenor, J., Marri, L., Buttner, M.J., and Thompson, C.J. (2001) A connection between stress and development in the multicellular prokaryote *Streptomyces coelicolor* A3(2). *Mol Microbiol* **40**: 804–814.
- Kieser, T., Bibb, M.J., Buttner, M.J., Chater, K.F., and Hopwood, D.A. (2000) *Practical Streptomyces Genetics*. Norwich: The John Innes Foundation.
- Kim, B., and Little, J.W. (1993) LexA and lambda CI repressors as enzymes: specific cleavage in an intermolecular reaction. *Cell* **73**: 1165–1173.
- Kim, I.K., Kim, M.K., Lee, C.J., Yim, H.S., Cha, S.S., and Kang, S.O. (2004) Crystallization and preliminary X-ray crystallographic analysis of the DNA-binding domain of BldD from *Streptomyces coelicolor* A3(2). *Acta Crystallogr Sect D Biol Crystallogr* **60**: 1115–1117.
- Kodani, S., Hudson, M.E., Durrant, M.C., Buttner, M.J., Nodwell, J.R., and Willey, J.M. (2004) The SapB morphogen is a lantibiotic-like peptide derived from the product of the developmental gene *ramS*. *Streptomyces coelicolor*. *Proc Natl Acad Sci USA* **101**: 11448–11453.
- Laskowski, R.A., MacArthur, M.W., Moss, D.S., and Thornton, J.M. (1993) PROCHECK: a program to check the stereochemical quality of protein structures. *J Appl Crystallogr* **26**: 283–291.
- Lewis, R.J., Brannigan, J.A., Offen, W.A., Smith, I., and Wilkinson, A.J. (1998) An evolutionary link between sporulation and prophage induction in the structure of a repressor: anti-repressor complex. *J Mol Biol* **283**: 907–912.
- Ma, H., and Kendall, K. (1994) Cloning and analysis of a gene cluster from *Streptomyces coelicolor* that causes accelerated aerial mycelium formation in *Streptomyces lividans*. *J Bacteriol* **176**: 3800–3811.
- Maniatis, T., and Ptashne, M. (1973) Multiple repressor binding at the operators in bacteriophage lambda. *Proc Natl Acad Sci USA* **70**: 1531–1535.
- Maniatis, T., Ptashne, M., Backman, K., Kield, D., Flashman, S., Jeffrey, A., and Maurer, R. (1975) Recognition sequences of repressor and polymerase in the operators of bacteriophage lambda. *Cell* **5**: 109–113.
- Merrick, M.J. (1976) A morphological and genetic mapping study of bald colony mutants of *Streptomyces coelicolor*. *J General Microbiol* **96**: 299–315.
- Meyer, B.J., Maurer, R., and Ptashne, M. (1980) Gene regulation at the right operator (OR) of bacteriophage lambda. II. OR1, OR2, and OR3: their roles in mediating the effects of repressor and cro. *J Mol Biol* **139**: 163–194.
- Molle, V., and Buttner, M.J. (2000) Different alleles of the response regulator gene *blbM* arrest *Streptomyces coelicolor* development at distinct stages. *Mol Microbiol* **36**: 1265–1278.
- Nam, G.H., Jang, D.S., Cha, S.S., Lee, T.H., Kim, D.H., Hong, B.H., et al. (2001) Maintenance of alpha-helical structures by phenyl rings in the active-site tyrosine triad contributes to catalysis and stability of ketosteroid isomerase from *Pseudomonas putida* biotype B. *Biochemistry* **40**: 13529–13537.
- Nodwell, J.R., McGovern, K., and Losick, R. (1996) An oligopeptide permease responsible for the import of an extracellular signal governing aerial mycelium formation in *Streptomyces coelicolor*. *Mol Microbiol* **22**: 881–893.
- Nodwell, J.R., Yang, M., Kuo, D., and Losick, R. (1999) Extracellular complementation and the identification of additional genes involved in aerial mycelium formation in *Streptomyces coelicolor*. *Genetics* **151**: 569–584.
- O'Connor, T.J., Kanellis, P., and Nodwell, J.R. (2002) The *ramC* gene is required for morphogenesis in *Streptomyces coelicolor* and expressed in a cell type-specific manner under the direct control of RamR. *Mol Microbiol* **45**: 45–57.
- Otwinowski, Z., and Minor, W. (1997) Processing of X-ray diffraction data collected in oscillation mode. *Meth Enzymol* **276**: 307–326.
- Page, M.S., Leibovitz, E., and Buttner, M.J. (1999) Evidence that the extracytoplasmic function sigma factor  $\sigma^E$  is

- required for normal cell wall structure in *Streptomyces coelicolor* A3(2). *J Bacteriol* **181**: 204–211.
- Pope, M.K., Green, B.D., and Westpheling, J. (1996) The *bld* mutants of *Streptomyces coelicolor* are defective in the regulation of carbon utilization, morphogenesis and cell–cell signalling. *Mol Microbiol* **19**: 747–756.
- Roberts, J.W., and Roberts, C.W. (1975) Proteolytic cleavage of bacteriophage lambda repressor in induction. *Proc Natl Acad Sci USA* **72**: 147–151.
- Sekharudu, C., Ramakrishnan, B., Huang, B., Jiang, R.T., Dupureur, C.M., Tsai, M.D., and Sundaralingam, M. (1992) Crystal structure of the Y52F/Y73F double mutant of phospholipase A2: increased hydrophobic interactions of the phenyl groups compensate for the disrupted hydrogen bonds of the tyrosines. *Protein Sci* **1**: 1585–1594.
- Serrano, L., Bycroft, M., and Fersht, A.R. (1991) Aromatic–aromatic interactions and protein stability. Investigation by double-mutant cycles. *J Mol Biol* **218**: 465–475.
- Terwilliger, T.C. (1999) Reciprocal-space solvent flattening. *Acta Crystallogr Sect D Biol Crystallogr* **55**: 1863–1871.
- Terwilliger, T.C., and Berendzen, J. (1999) Discrimination of solvent from protein regions in native Fouriers as a means of evaluating heavy-atom solutions in the MIR and MAD methods. *Acta Crystallogr Sect D Biol Crystallogr* **55**: 501–505.
- Tillotson, R.D., Wosten, H.A., Richter, M., and Willey, J.M. (1998) A surface active protein involved in aerial hyphae formation in the filamentous fungus *Schizophyllum commune* restores the capacity of a bald mutant of the filamentous bacterium *Streptomyces coelicolor* to erect aerial structures. *Mol Microbiol* **30**: 595–602.
- Willey, J., Santamaria, R., Guijarro, J., Geistlich, M., and Losick, R. (1991) Extracellular complementation of a developmental mutation implicates a small sporulation protein in aerial mycelium formation by *S. coelicolor*. *Cell* **65**: 641–650.
- Willey, J., Schwedock, J., and Losick, R. (1993) Multiple extracellular signals govern the production of a morphogenetic protein involved in aerial mycelium formation by *Streptomyces coelicolor*. *Genes Dev* **7**: 895–903.
- Wintjens, R., and Rooman, M. (1996) Structural classification of HTH DNA-binding domains and protein–DNA interaction modes. *J Mol Biol* **262**: 294–313.